Tensile properties of graphene nanotube hybrid structures: a molecular dynamics study

H.F. Zhan, K. Xia and Y.T. Gu*

School of Chemistry, Physics and Mechanical Engineering, *Queensland University of Technology, Brisbane, QLD 4001, Australia*

*Corresponding author: yuantong.gu@qut.edu.au

Abstract

Graphene has been reported with record-breaking properties which have opened up huge potential applications. A considerable research has been devoted to manipulate or modify the properties of graphene to target a more smart nanoscale device. Graphene and carbon nanotube hybrid structure (GNHS) is one of the promising graphene derivates, while their mechanical properties have been rarely discussed in literature. Therefore, such a studied is conducted in this paper basing on the large-scale molecular dynamics simulation. The target GNHS is constructed by considering two separate graphene layers that being connected by single-wall carbon nanotubes (SWCNTs) according to the experimental observations. It is found that the GNHSs exhibit a much lower yield strength, Young's modulus, and earlier yielding comparing with a bilayer graphene sheet. Fracture of studied GNHSs is found to fracture located at the connecting region between carbon nanotubes (CNTs) and graphene. After failure, monatomic chains are normally observed at the front of the failure region, and the two graphene layers at the failure region without connecting CNTs will adhere to each other, generating a bilayer graphene sheet scheme (with a layer distance about 3.4 Å). This study will enrich the current understanding of the mechanical performance of GNHS, which will guide the design of GNHS and shed lights on its various applications.

Keywords: graphene, nanotube, tension, Young's modulus, molecular dynamics simulation

Introduction

The carbon nanotube (CNT) and graphene have grabbed appreciable scientific community attentions, owning to their excellent performance in the field of mechanics, photology, electronics and bio-sensing (Zhu et al. 2010; Wang 2005). Their record-breaking properties (e.g., enormous Young's modulus, fracture strength and low mass density) have enabled them with a wide promising applications in the nanoelectromechanical system (NEMS) including force, mass and position sensors, bio-sensors as well as high frequency resonators (Chen et al. 2009). Synthesising these two nanomaterials together, a graphene and nanotube hybrid structure (GNHS) is formed, which can be used to fabricate field-emitter devices and double layer capacity, demonstrating much improved performance over pervious designed CNT-bulk metal structures (Yan et al. 2012). Specifically, a combination of nanotube

and graphene layer extends the electric conductivity to three dimensions, which shows promising applications in solar cells (Yen et al. 2011; Wang, Zhi and Müllen 2008).

It is noticed that several works have been devoted to investigate the electrical and thermal properties of GNHS (Zhu et al. 2012; Varshney et al. 2010; Novaes, Rurali and Ordejón 2010), while the studies of the mechanical performance, stability or durability of the hybrid structure are still lacking in literature. Typically, one relies on either experiments or numerical simulations to probe the mechanical properties of nanomaterials. While, it is generally accepted that experimental approach is usually suffering from several shortages, such as huge manipulation complex and experimental uncertainties. On the other hand, numerical simulation has been witnessed as an effective and efficient tool in investigating the performance and properties of nanomaterials or nano-device (Zhan and Gu 2011; Gu and Zhan 2012; Zhan, Gu and Park 2012), which could compensate certain experimental shortages, e.g., provides atomic-resolution deformation process of the material under loading in a degree of detail not possible experimentally.

Therefore, in this work, the molecular dynamics (MD) simulation, as one of the popular simulation approaches, will be employed to unveil the tensile performance of GNHS. Emphasis will be placed on the Young's modulus, as well as the yield strength of different GNHSs that are constructed with different allocations of CNTs.

Computational details

A series of large-scale MD simulations were carried out to investigate how the GNHS will perform when different allocations of CNTs are applied to connect two separate graphene layers. After several papers are viewed (Matsumoto and Saito 2002; Dimitrakakis, Tylianakis and Froudakis 2008; Novaes, Rurali and Ordejón 2010; Varshney et al. 2010), a specific cylindrical hole is made on the graphene to fit the selected CNT, which is armchair (4, 4) CNT with a height of 13.8 Å in our case. Different testing samples have an almost identical size around 24.7×5.6 nm^2. Basically, five different allocations of CNTs have been used, including a rectangular allocation with 10 CNTs (denoted as R10-GNHS, shown in Fig. 1a), 12 CNTs (denoted as R12-GNHS) and 14 CNTs (denoted as R14-GNHS), a triangular allocation of 12 CNTs (denoted as T12-GNHS, shown in Fig. 1b) and 17 CNTs (denoted as T17-GNHS, shown in Fig. 1c).

In the MD simulation, the popularly applied reactive empirical bond order (REBO) potential (Brenner et al. 2002) was adopted to describe the interactions of C atoms, which has been shown to well represent the binding energy and elastic properties of graphene and CNT (Zhang et al. 2011). During the simulation, the GNHS was firstly relaxed to a minimum energy state using the conjugate gradient algorithm. We then used the Nose-Hoover thermostat (Hoover 1985; Nosé 1984) to equilibrate the GNHS at 1 K (NVT ensemble) for 500 ps at a time step of 1 fs. Finally, a constant velocity of

0.001 Å/ps was applied to one end of the GNHS along the length direction (*y*-axis in Fig. 1), while holding another end fixed. The equations of motion are integrated with time using a Velocity Verlet algorithm (Verlet 1967). No periodic boundary conditions have been applied. The system temperature was maintained at 1 K during the simulation to minimize the influence from thermal fluctuations. All simulations were performed using the open-source LAMMPS code (Plimpton 1995).

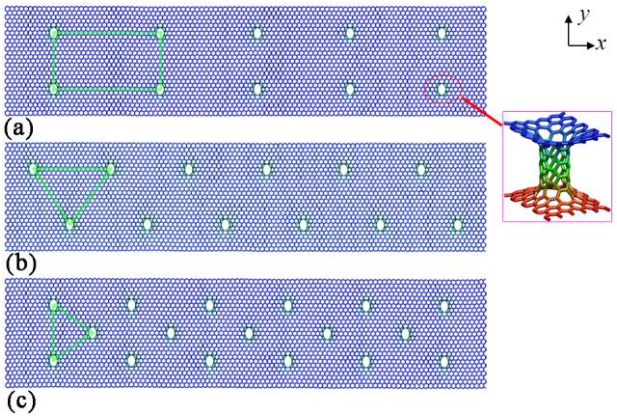

Figure 1. Simulation models of different GNHSs. (a) A rectangular allocation of 10 CNTs between two separate graphene layers; (b) A triangular allocation of 12 CNTs; (c) A triangular allocation of 17 CNTs. Inset shows the bonds between graphene layer and CNT.

Results and discussion

In the following, the tensile properties that extracted from the stress-strain curves will be discussed among different cases. Specifically, Young's modulus *E* will be calculated as the initial slope of the stress-strain curve within a strain of 5%. The yield strength and fracture strain are defined at the point where the peak stress is arrived. For the purpose of comparison and also validation, we studied the tensile properties of a bilayer graphene at the beginning. Figure 2a shows the simulation results for a bilayer GS. Young's modulus and the yield strength are estimated as 0.96 TPa and 128 GPa, respectively, which are consistent with that reported by previous researchers (Zhang et al. 2011). Figures 2b and 2c present the atomic configurations of the bilayer GS before and after failure, respectively. As is seen in Figure 2b, during the elastic deformation period, all the C-C bonds have been stretched in the loading direction. With the increasing strain, initial failure is found at the two edges of the bilayer GS which is caused by the bond breaking processes. Since the appearance of these breaking bonds, the bilayer GS is found to fail quickly as indicated by the sharp decrease of the stress after yield strain, signifying a brittle behaviour. It is found that after the failure of the sample, several short monatomic chains are formed at the front of the failure region, as shown in inset of Figure 2c.

We then turned to the tensile properties of different GNHSs. Figure 3 presents the stress-strain curves obtained from the MD simulations. Comparing with the bilayer

GS, an evident decrease of the yield strength and early yielding are observed. Rather than a nonlinear stress-strain curve of the bilayer GS at a higher strain during the elastic deformation region (shown in Figure 2), all GNHSs exhibit a linear stress-strain curve during the whole elastic deformation period. The brittle failure phenomenon is also observed in different GNHSs as indicated by the sharp decrease of stress after yielding in Figure 3.

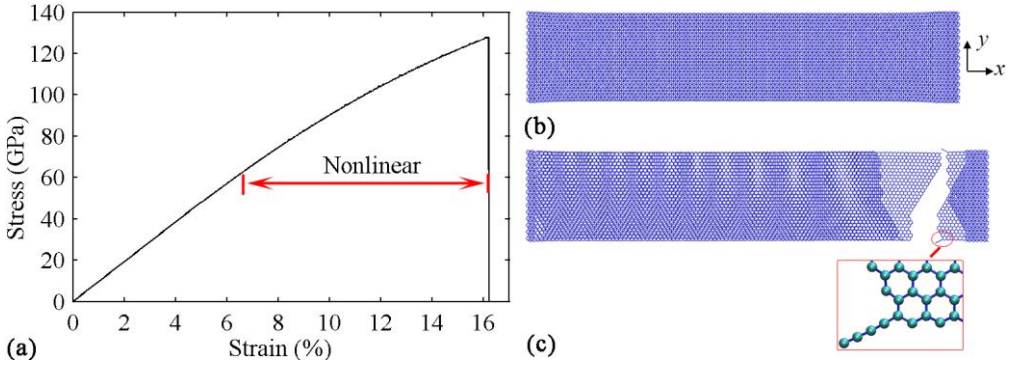

Figure 2. Numerical results from a bilayer GS: (a) Stress-strain curve; (b) Atomic configuration at 1996 ps; (c) Atomic configuration at 3870 ps. Inset shows the monatomic chain at the front of the failure region.

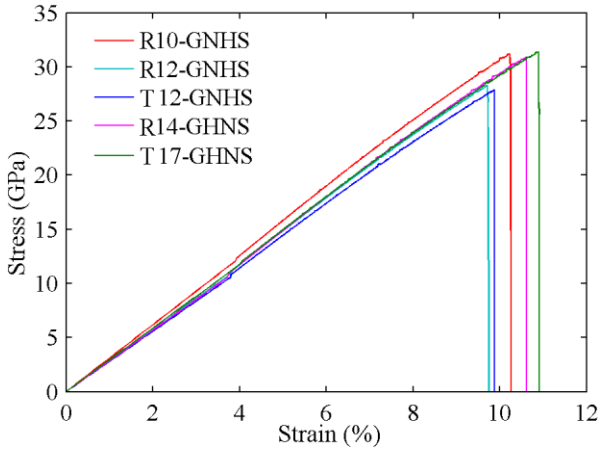

Figure 3. Stress-strain curves obtained from five different graphene and nanotube hybrid structures (GNHSs).

The tensile properties of different GNHSs are summarised in Table 1. As aforementioned, a relatively smaller yield strength and earlier yielding are found in these GNHSs comparing with that of a bilayer GS. Specifically, the T12-GNHS exhibit the smallest yield strength of ~27.88 GPa, which is only one fifth of bilayer GS's yield strength. Other four GNHSs also exhibit a similar low yield strength. In the other hand, the R12-GNHS shows the earliest yielding, at a strain of 9.71%, followed by the T12-GNHS with the yield strain as 9.88%. According to the results from the three GNHSs with rectangular allocations of CNTs, more connecting CNTs does not necessary mean a superior tensile property. While for the rest two cases with triangular allocation, better tensile properties are found for the one with more CNTs,

i.e., T17-GNHS. It can be concluded that the tensile properties of GNHS is determined by both the number and allocation schemes of the connecting CNTs.

Table 1. Tensile properties of different GNHSs.

	Bilayer GS	R10-GNHS	R12-GNHS	T12-GNHS	R14-GNHS	T17-GNHS
Yield strength (GPa)	127.88	31.21	28.30	27.88	30.88	31.38
Yield strain (%)	16.12	10.23	9.71	9.88	10.60	10.90
Young's modulus (TPa)	0.96	0.31	0.28	0.28	0.28	0.29

To acquire the in-detail influence that induced by different allocations of CNTs, the atomic configurations of different GNHSs are compared at different simulation time. Figures 4a - 4d illustrate the atomic configuration of the R10-GNHS before and after failure. As illustrated in Figure 4a, the C-C bond that connecting the CNT and graphene is broken due to the high tensile strain. From Figure 4b, the fracture is occurred around the two connecting CNTs, and other CNTs that are adjacent to the fracture region are tilted by the tensile strain. Similar as the bilayer GS, several monatomic chains are formed at the failure region as revealed in Figure 4c. It is worth noting that the two GS layers adhere to each other because of the absence of connecting CNTs after fracture, which induce a local bilayer GS scheme with the initial layer distance reducing from the original 13.8 Å to approximate 3.4 Å. Such deformation processes are observed in other GNHSs with rectangular allocation of CNTs, i.e., R12-GNHS, R14-GNHS.

Simulation results have shown that the triangular allocation of CNT will endow the hybrid structure with different tensile behaviours. As presented in Figures 4f, for the T12-GNHS, more connecting CNTs have been tilted due to the increasing tensile stress, and the fracture occur around two CNTs. After fracture, two monatomic chain circles are formed at the locations of the corrupted CNTs, as shown in Figure 4g. Unlike previous cases with rectangular allocation of CNTs where the two graphene layers broke nearly at the same location, the two graphene layers of the T12-GNHS fracture differently as illustrated in Figure 4g. Consistently, we found the two graphene layers adhere to each other at the failure region due to the rupture of the connecting CNT.

Interestingly, for the T17-GNHS, the fracture is occurred around the region with two connecting CNTs rather than the area with only one CNT. After fracture, several monatomic chains are formed as illustrated in Figure 5c. We note that, the two CNTs have been spilt into two parts rather than rupture in previous cases, which leads the two GS layers still being separated with a relatively large distance (see Figure 5d). According to above discussions, it is concluded that the two GS layers connected by

CNTs will exhibit a much lower yield strength, Young's modulus and earlier yielding than a normal bilayer GS. The fracture or failure is usually occurred around the locations of connecting CNTs and the monatomic chains are normally observed at the failure region. Comparing with a bilayer GS, more monatomic chains are formed in the hybrid structures after yielding due to the failure of CNTs.

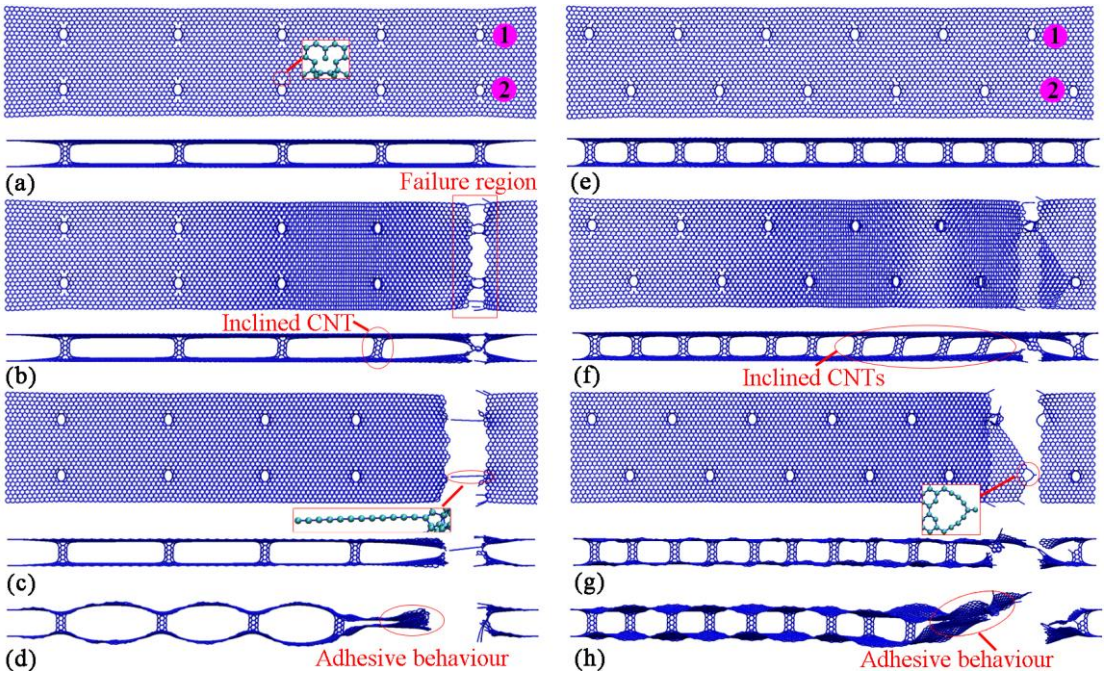

Figure 4. Atomic configurations of HGNSs at different simulation time. R10-GNHS at: (a) 2562 ps, inset shows the broken C-C bonds around the connecting CNT, (b) 2568 ps, (c) 2586 ps, inset shows the formation of a monatomic chain, (d) 2616 ps; T12-GNHS at: (e) 2052 ps, (f) 2508 ps, inset shows the formation of a monatomic chain circle, (g) 2532 ps, (h) 2556 ps.

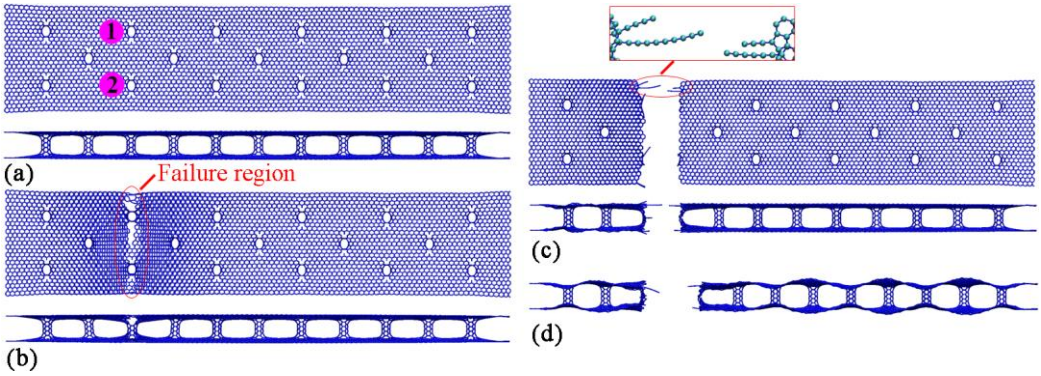

Figure 5. Atomic configurations of the T17-GNHS at different simulation time: (a) 2216 ps, (b) 2692 ps, (c) 2706 ps, inset shows the formation of four monatomic chains, (d) 2724 ps.

Conclusions

Basing on the large-scale MD simulation, the tensile properties of graphene carbon nanotube hybrids structures have been investigated. Discussions are emphasised on the yield strength, Young's modulus and the failure mechanisms. It is found that the GNHSs exhibit a much lower yield strength, Young's modulus, and earlier yielding comparing with a bilayer GS. Particularly, fracture of studied GNHSs is found to locate around connecting regions between CNTs and graphene. After failure, monatomic chains are normally observed at the front of the failure region, and the two graphene layers at the failure region without connecting CNTs will adhere to each other to generate a local bilayer GS scheme (i.e., the distance of the two layers reduces to a value of ~ 3.4 Å). This study provides a fundamental investigation of the tensile properties of the graphene nanotube hybrid structures, which will benefit the design and also the applications of graphene-based hybrid materials.

Acknowledgements

Support from the ARC Discovery Project (DP130102120) and the High Performance Computer resources provided by the Queensland University of Technology are gratefully acknowledged.

References

Brenner, Donald W, Olga A Shenderova, Judith A Harrison, Steven J Stuart, Boris Ni and Susan B Sinnott. 2002. "A second-generation reactive empirical bond order (REBO) potential energy expression for hydrocarbons." *Journal of Physics: Condensed Matter* 14 (4): 783.

Chen, Changyao, Sami Rosenblatt, Kirill I Bolotin, William Kalb, Philip Kim, Ioannis Kymissis, Horst L Stormer, Tony F Heinz and James Hone. 2009. "Performance of monolayer graphene nanomechanical resonators with electrical readout." *Nature nanotechnology* 4 (12): 861-867.

Dimitrakakis, Georgios K, Emmanuel Tylianakis and George E Froudakis. 2008. "Pillared graphene: a new 3-D network nanostructure for enhanced hydrogen storage." *Nano letters* 8 (10): 3166-3170.

Gu, Y. T. and H. F. Zhan. 2012. "MD investigations for mechanical properties of copper nanowires with and without surface defects " *International Journal of Computational Methods* 9 (1): 1240003.

Hoover, W.G. 1985. "Canonical dynamics: Equilibrium phase-space distributions." *Physical Review A* 31 (3): 1695-1697.

Matsumoto, Takanori and Susumu Saito. 2002. "Geometric and electronic structure of new carbon-network materials: Nanotube array on graphite sheet." *Journal of the Physical Society of Japan* 71: 2765.

Nosé, S. 1984. "A unified formulation of the constant temperature molecular dynamics methods." *The Journal of Chemical Physics* 81: 511.

Novaes, Frederico D, Riccardo Rurali and Pablo Ordejón. 2010. "Electronic transport between graphene layers covalently connected by carbon nanotubes." *ACS nano* 4 (12): 7596-7602.

Plimpton, S. 1995. "Fast parallel algorithms for short-range molecular dynamics." *Journal of Computational Physics* 117 (1): 1-19.

Varshney, Vikas, Soumya S Patnaik, Ajit K Roy, George Froudakis and Barry L Farmer. 2010. "Modeling of thermal transport in pillared-graphene architectures." *ACS nano* 4 (2): 1153-1161.

Verlet, Loup. 1967. "Computer 'experiments' on classical fluids. I. Thermodynamical Properties of Lennard-Jones Molecules." *Physical Review* 159: 98-103.

Wang, Joseph. 2005. "Carbon - nanotube based electrochemical biosensors: A review." *Electroanalysis* 17 (1): 7-14.

Wang, Xuan, Linjie Zhi and Klaus Müllen. 2008. "Transparent, conductive graphene electrodes for dye-sensitized solar cells." *Nano letters* 8 (1): 323-327.

Yan, Zheng, Lulu Ma, Yu Zhu, Indranil Lahiri, Myung Gwan Hahm, Zheng Liu, Shubin Yang, Changsheng Xiang, Wei Lu and Zhiwei Peng. 2012. "Three-Dimensional Metal–Graphene–Nanotube Multifunctional Hybrid Materials." *ACS nano* 7 (1): 58-64.

Yen, Ming-Yu, Min-Chien Hsiao, Shu-Hang Liao, Po-I Liu, Han-Min Tsai, Chen-Chi M Ma, Nen-Wen Pu and Ming-Der Ger. 2011. "Preparation of graphene/multi-walled carbon nanotube hybrid and its use as photoanodes of dye-sensitized solar cells." *Carbon* 49 (11): 3597-3606.

Zhan, H.F. and Y.T. Gu. 2011. "Atomistic exploration of deformation properties of copper nanowires with pre-existing defects." *CMES: Computer Modeling in Engineering & Sciences* 80 (1): 23-56.

Zhan, Haifei, Yuantong Gu and Harold S. Park. 2012. "Beat phenomena in metal nanowires, and their implications for resonance-based elastic property measurements." *Nanoscale* 4 (21): 6779-6785.

Zhang, YY, CM Wang, Y. Cheng and Y. Xiang. 2011. "Mechanical properties of bilayer graphene sheets coupled by sp^3 bonding." *Carbon* 49 (13): 4511-4517.

Zhu, Yanwu, Shanthi Murali, Weiwei Cai, Xuesong Li, Ji Won Suk, Jeffrey R Potts and Rodney S Ruoff. 2010. "Graphene and graphene oxide: synthesis, properties, and applications." *Advanced Materials* 22 (35): 3906-3924.

Zhu, Yu, Lei Li, Chenguang Zhang, Gilberto Casillas, Zhengzong Sun, Zheng Yan, Gedeng Ruan, Zhiwei Peng, Abdul-Rahman O Raji and Carter Kittrell. 2012. "A seamless three-dimensional carbon nanotube graphene hybrid material." *Nature Communications* 3: 1225.